The Relationship between Aristotelian and Hasse Diagrams

Lorenz Demey[1] and Hans Smessaert[2]

[1] Center for Logic and Analytic Philosophy, KU Leuven
Lorenz.Demey@hiw.kuleuven.be
[2] Department of Linguistics, KU Leuven
Hans.Smessaert@arts.kuleuven.be

Abstract. The aim of this paper is to study the relationship between two important families of diagrams that are used in logic, viz. Aristotelian diagrams (such as the well-known 'square of oppositions') and Hasse diagrams. We discuss some obvious similarities and dissimilarities between both types of diagrams, and argue that they are in line with general cognitive principles of diagram design. Next, we show that a much deeper connection can be established for Aristotelian/Hasse diagrams that are closed under the Boolean operators. We consider the Boolean algebra $\mathbb{B}_n$ with 2^n elements, whose Hasse diagram can be drawn as an n-dimensional hypercube. Both the Aristotelian *and* the Hasse diagram for $\mathbb{B}_n$ can be seen as $(n-1)$-dimensional vertex-first projections of this hypercube; whether the diagram is Aristotelian or Hasse depends on the projection axis. We show how this account provides a unified explanation of the (dis)similarities between both types of diagrams, and illustrate it with some well-known Aristotelian/Hasse diagrams for $\mathbb{B}_3$ and $\mathbb{B}_4$.

Keywords: Aristotelian diagram, Hasse diagram, square of oppositions, logical geometry, hexagon, rhombic dodecahedron, hypercube.

1 Introduction

Logicians make use of several kinds of diagrams for a variety of purposes, such as obtaining new results and communicating their findings more effectively. Roughly, the diagrams used in logic can be divided into two broad classes. On the one hand, there are diagrams that visualize formulas from some given logical system; typical examples include Euler diagrams, Venn diagrams, spider diagrams, Peirce's existential graphs, etc. [1–5]. In these cases, one diagram visualizes a single formula, and visual operations on the diagram correspond to logical operations on that formula. Diagrammatic reasoning thus consists in a sequence of operations that gradually transforms an initial diagram into another diagram. On the other hand, logicians also use diagrams to visualize certain *relations* between formulas from some given logical system. Typical examples include Aristotelian diagrams, Hasse diagrams and duality diagrams [6–13]. In these cases, one diagram contains several formulas, and diagrammatic reasoning

consists in 'traversing' the diagram by making use of the relations between the formulas.[1] Since the focus is on the relations between the formulas, the formulas themselves are usually simply visualized as symbolic labels attached to the vertices in the diagram.[2]

The aim of this paper is to study the relationship between two main types of diagrams of the second class, viz. Aristotelian and Hasse diagrams. On the one hand, there are some obvious similarities between these two types; for example, the relation of logical implication (also called subalternation or entailment) is visualized in Aristotelian as well as Hasse diagrams. On the other hand, there are also some equally obvious dissimilarities; for example, in Hasse diagrams, the implications all go in the same general direction (viz. upwards), but in Aristotelian diagrams, they tend to go in a wide variety of directions. Because of this equivocal evidence, the overall picture of the relationship between Aristotelian and Hasse diagrams has remained unclear up till now.

However, in this paper, we show that there exists a deep connection between these two types of diagrams. On a *visual-cognitive* level, we argue that their dissimilarities can perfectly be explained in terms of general principles of diagram design and information visualization. Next, on a more abstract *geometrical* level, we show that if we restrict ourselves to Boolean closed diagrams, Aristotelian and Hasse diagrams can be seen as different vertex-first projections of one and the same hypercube (whether the resulting diagram is Aristotelian or Hasse depends on the projection axis). This account naturally yields a unified explanation of the obvious similarities and dissimilarities mentioned above. Finally, these results are illustrated by means of some well-known Aristotelian and Hasse diagrams, such as the hexagon and the rhombic dodecahedron (RDH).

The paper is organized as follows. Section 2 formally introduces Aristotelian and Hasse diagrams, and briefly discusses their importance and usage in logic. Next, Section 3 examines some obvious similarities and dissimilarities between both kinds of diagrams, and relates them to general principles of diagram design. Section 4 contains the more technical results of this paper: it shows how Aristotelian and Hasse diagrams can be seen as vertex-first projections of hypercubes, and discusses how this leads to a unified explanation of the (dis)similarities between both types of diagrams. The next two sections illustrate these results by applying them to some well-known Aristotelian and Hasse diagrams, viz. the hexagon (Section 5) and the RDH (Section 6). Finally, Section 7 wraps things up, and mentions some questions that are left for further research.

---

[1] For example, most readers will be familiar with the reasoning task in which one is presented with a square of oppositions and the truth value of (the formula in) one of the square's corners, and is then asked to determine the truth values of the other corners by making use of the Aristotelian relations [14, Exercise 4.5.I].

[2] However, there also exist Aristotelian/Hasse diagrams in which the formulas themselves are visualized as diagrams as well. For example, Bernhard [15] discusses a multi-layered square of opposition in which the four formulas are visualized as small Euler/Venn diagrams that are embedded inside a large Aristotelian diagram.

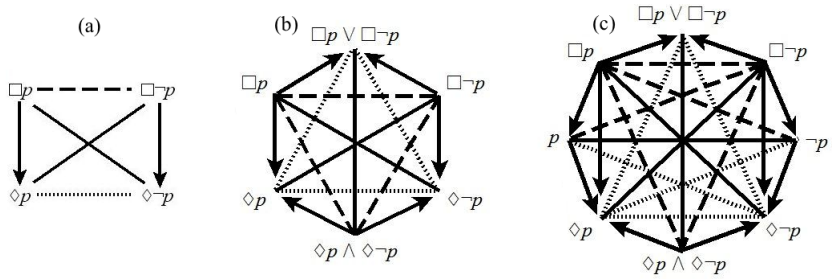

Fig. 1. Aristotelian (a) square, (b) hexagon and (c) octagon for the modal logic S5

2 Aristotelian and Hasse Diagrams

An Aristotelian diagram visualizes a set of logical formulas and the Aristotelian relations between them. These relations are defined as follows (relative to some given logical system S, which is supposed to have the usual Boolean connectives): the formulas φ and ψ are said to be

contradictory	iff	$\mathsf{S} \models \neg(\varphi \wedge \psi)$	and	$\mathsf{S} \models \neg(\neg\varphi \wedge \neg\psi)$,
contrary	iff	$\mathsf{S} \models \neg(\varphi \wedge \psi)$	and	$\mathsf{S} \not\models \neg(\neg\varphi \wedge \neg\psi)$,
subcontrary	iff	$\mathsf{S} \not\models \neg(\varphi \wedge \psi)$	and	$\mathsf{S} \models \neg(\neg\varphi \wedge \neg\psi)$,
in subalternation	iff	$\mathsf{S} \models \varphi \rightarrow \psi$	and	$\mathsf{S} \not\models \psi \rightarrow \varphi$.

Furthermore, almost all Aristotelian diagrams that have appeared in the literature impose the following additional constraints on the formulas that are visualized: these formulas are (i) contingent and (ii) pairwise non-equivalent, and (iii) they come in contradictory pairs (i.e. for a given formula φ, the diagram contains both φ and $\neg\varphi$). Finally, almost all Aristotelian diagrams are centrally symmetric, with all contradictory pairs ordered around the center of symmetry (so that φ is diametrically opposed to $\neg\varphi$).

The most widely known Aristotelian diagram is of course the so-called 'square of oppositions'. This diagram has a rich tradition [16, Chapter 5], but it is also widely used by contemporary logicians to visualize interesting fragments of systems such as modal logic [17], (dynamic) epistemic logic [8, 18] and deontic logic [19, 20]. There is also a vast literature on Aristotelian diagrams other than the traditional square. The most widely known among these is probably the hexagon proposed by Jacoby, Sesmat and Blanché [21–23], but several other hexagons, octagons, etc. have been studied in detail [10, 16, 24]. Figure 1 shows an Aristotelian square, hexagon and octagon for the modal logic S5.[3]

We now turn to the second type of diagrams, viz. Hasse diagrams. In general, these are used to visualize partially ordered sets (posets). A poset consists of a set

[3] There is no universally accepted way of visualizing the Aristotelian relations. We here follow the convention introduced in [12], and visualize the relations of contradiction, contrariety, subcontrariety and subalternation by means of a full line (—), a dashed line (- - -), a dotted line (· · ·) and an arrow (⟶), respectively.

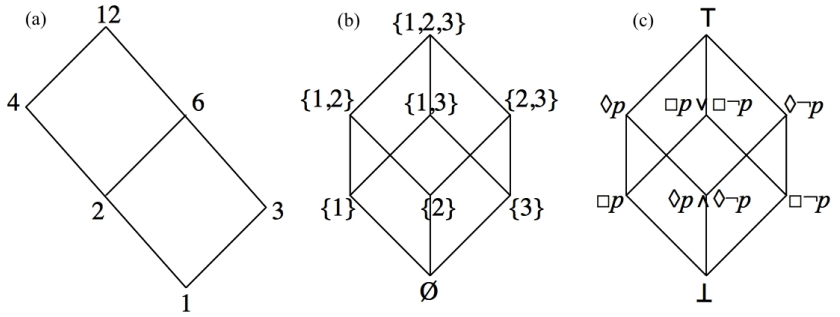

Fig. 2. Hasse diagrams for (a) the divisors of 12, (b) the Boolean algebra $\wp(\{1,2,3\})$, and (c) a Boolean algebra of formulas from the modal logic S5

P and a partial ordering $\leq$, i.e. a binary relation on P that is reflexive, transitive, and antisymmetric. If $x \leq y$ and not $y \leq x$, we say that $x < y$. If $x < y$ and there is no $z \in P$ such that $x < z < y$, we say that $x \lhd y$. A Hasse diagram visualizes the poset $(P, \leq)$ in such a way that if $x \lhd y$, the point representing x is connected by a line segment to the point representing y (furthermore, y should be 'above' x, so that the line segment from x to y runs upwards) [6].

Hasse diagrams have a wide variety of applications. Typical examples from mathematics include divisibility posets (in which $x \leq y$ iff x divides y) and subgroup lattices [6]; more practical applications come from formal concept analysis [25]. In this paper, however, we will focus on their applications in logic, and thus assume that the underlying poset (with $\leq$ being logical entailment) is a Boolean algebra, i.e. has top and bottom elements, and meet, join and complementation operations. It is well-known that a Boolean algebra can always be visualized by means of a Hasse diagram that is centrally symmetric (with all complementary pairs of elements ordered around the center of symmetry) [6]. Furthermore, a finite Boolean algebra can be partitioned into 'levels' $L_0, L_1, L_2, \ldots$, which are recursively defined as follows: $L_0 = \{\bot\}$, and $L_{k+1} = \{x \mid \exists y \in L_k : y \lhd x\}$. Figure 2 shows Hasse diagrams for the divisors of 12, the Boolean algebra $\wp(\{1,2,3\})$, and a Boolean algebra of formulas from the modal logic S5.

To fully appreciate the results that will be presented in Section 4, it should be realized that although most Aristotelian and Hasse diagrams are two-dimensional, this restriction is certainly not essential. In recent years, several three-dimensional Aristotelian diagrams have been studied, such as octahedrons, cubes, RDHs, etc. [8, 9, 26–28]. Similarly, there have also been studies on three-dimensional Hasse diagrams, such as (hyper)cubes and RDHs [13, 29–31].[4] Figure 3 shows

[4] Recalling the typology of logic diagrams presented in Section 1, it should be noted that the trend towards three-dimensional diagrams includes not only Aristotelian and Hasse diagrams, but also other diagrams that visualize relations between formulas (e.g. duality diagrams [7]), and even diagrams that visualize single formulas (e.g. Euler and Venn diagrams [32]).

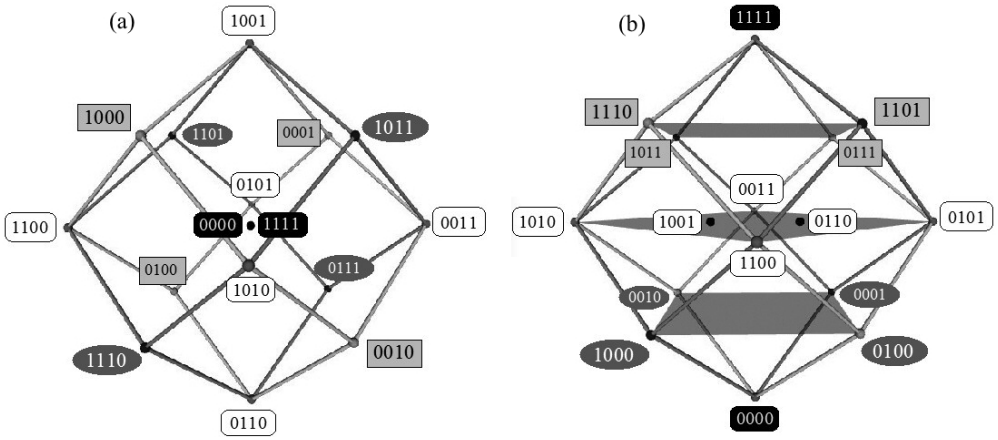

Fig. 3. (a) Aristotelian and (b) Hasse rhombic dodecahedron for CPL

an Aristotelian and a Hasse RDH for the binary, truth-functional connectives of classical propositional logic (CPL); each connective is identified with its truth table (for example, conjunction is written as 1000, disjunction as 1110, etc.).

3 Similarities, Dissimilarities, and Diagram Design

We now discuss some obvious similarities and dissimilarities between Aristotelian and Hasse diagrams, and explain how they relate to general cognitive principles of diagram design and information visualization.

Let's start with the similarities between Aristotelian and Hasse diagrams. First of all, it should be noted that both types of diagrams represent the formulas *up to logical equivalence*, i.e. if φ and ψ are logically equivalent, then they cannot appear as distinct formulas in either type of diagram. In the case of a Hasse diagram for some Boolean logical system S, this is very clear: the poset that is visualized by the Hasse diagram is the Lindenbaum-Tarski algebra of S, whose elements are not individual formulas, but rather equivalence classes of formulas [6, p. 254ff.]. The literature on Aristotelian diagrams is less explicit about this logical equivalence condition (although there are exceptions [8, 12]), but nearly all Aristotelian diagrams that have been studied so far do indeed satisfy it.

A second, more important observation is that there is a large *overlap in the relations* visualized by the two types of diagrams. The Aristotelian relation of subalternation is identical to the notion of 'one-way entailment' $<$ (recall that $x < y$ iff $x \leq y$ and not $y \leq x$), which is itself the transitive closure of the covering relation $\lhd$ visualized by Hasse diagrams. Hence, if φ and ψ occur in an Aristotelian diagram D_1 and a Hasse diagram D_2, then there is a subalternation arrow from φ to ψ in D_1 iff there is an upward path (i.e. a sequence of $\lhd$-edges) from φ to ψ in D_2. Since all Aristotelian relations can be reduced to subalterna-

tion and contradiction,[5] and Hasse diagrams can represent these two relations (subalternation: just discussed; contradiction: by means of central symmetry), it follows that Hasse diagrams can represent all Aristotelian relations.

We now turn to the dissimilarities between Aristotelian and Hasse diagrams. The first difference concerns the *non-contingent formulas* $\bot$ and $\top$. These constitute the natural begin- and endpoints of the entailment ordering of a given Boolean logic S, and are thus visualized as resp. the lowest and the highest point of the Hasse diagram for S. This is the case regardless of whether this Hasse diagram happens to be two- or three-dimensional; for example, see the Hasse hexagon for $\mathsf{S5}$ in Fig. 2c and the Hasse RDH for CPL in Fig. 3b. In contrast, almost all Aristotelian diagrams that have appeared in the literature so far contain only contingent formulas. One possible explanation for this restriction is that $\bot$ and $\top$ enter into many 'vacuous' Aristotelian relations with contingent formulas,[6] which would only clutter the diagrams [8]. Although most Aristotelian diagrams do not represent the non-contingent formulas at all, some authors [27, 33] prefer to think of them as coinciding in the center of the diagram. From this perspective, $\bot$ and $\top$ still do not occupy any 'real' vertices of the diagram, but they are 'hidden' in its center of symmetry (which is itself *not* a separate vertex of the diagram); for example, see the Aristotelian RDH in Fig. 3a, and the formulas $\bot = 0000$ and $\top = 1111$ coinciding in its center.

A second difference concerns the *general direction of the entailments*. We have seen above that entailment is visualized in both Aristotelian and Hasse diagrams (resp. as subalternation and as the transitive closure of the covering relation $\lhd$). By definition, all individual $\lhd$-edges in a Hasse diagram are directed upwards, and hence, all paths of such edges are also directed upwards. In Hasse diagrams, all entailments thus have the same general direction (viz. upwards). By contrast, in Aristotelian diagrams the subalternation arrows generally do not share a single direction.[7] Consider, for example, the Aristotelian hexagon in Fig. 1b: the subalternations starting in $\Diamond p \wedge \Diamond\neg p$ and those ending in $\Box p \vee \Box\neg p$ all have the same general direction (viz. upwards), but the subalternations from $\Box(\neg)p$ to $\Diamond(\neg)p$ run in the exact opposite direction (viz. downwards).

The third difference is related to the *visualization of the levels* of the Boolean algebra that the formulas are taken from. In a Hasse diagram, the levels L_k are visualized as hyperplanes that are orthogonal to the general entailment direction. Since this entailment direction is vertically upwards (cf. supra), the levels are horizontal hyperplanes. In Aristotelian diagrams, by contrast, there is generally a complete 'mixing' of levels. For example, compare the Aristotelian and Hasse hexagons for $\mathsf{S5}$ in Fig. 1b and 2c, and focus on the L_1-formulas $\Box p$, $\Diamond p \wedge \Diamond\neg p$ and $\Box\neg p$. In the Hasse hexagon, these formulas constitute a horizontal line,

[5] Writing CD and SA for contradiction and subalternation, respectively, we have that φ and ψ are contrary iff $SA(\varphi, \neg\psi)$ iff $\exists\theta\big(CD(\psi,\theta)$ and $SA(\varphi,\theta)\big)$, and similarly, φ and ψ are subcontrary iff $SA(\neg\varphi,\psi)$ iff $\exists\theta\big(CD(\varphi,\theta)$ and $SA(\theta,\psi)\big)$ [12, § 3.3.3].

[6] E.g. $\bot$ is contrary to every contingency, and $\top$ is subcontrary to every contingency.

[7] The main exception to this claim is, of course, the Aristotelian square, in which all subalternations are directed downwards; see Fig. 1a.

whereas in the Aristotelian hexagon, they constitute a triangle. Similarly, when comparing the RDHs for CPL, we see that the L_1-formulas 1000, 0100, 0010 and 0001 constitute a horizontal plane in the Hasse RDH in Fig. 3b (visualized in transparent grey), but a tetrahedron in the Aristotelian RDH in Fig. 3a.

The similarities and dissimilarities between Aristotelian and Hasse diagrams discussed above are fully in line with general principles about diagram design, such as *congruity*, *apprehension* and *information selection* [34, 35]. Both types of diagrams are used to visualize certain logical relations between formulas. Hasse diagrams primarily focus on the structure of the entailment ordering $<$, and try to establish a strong congruence between this logical structure and the visual structure of the diagram. For example, the Hasse hexagon in Fig. 2c visualizes the fact that $\Box p$ entails $\Diamond p$ by putting $\Box p$ lower than $\Diamond p$; similarly, it visualizes the fact that the L_1-formulas $\Box p$, $\Diamond p \wedge \Diamond \neg p$ and $\Box \neg p$ do not entail each other (and are thus *independent* with respect to the entailment ordering) by putting them on a line that is *orthogonal* to the direction of the entailment ordering.

From an Aristotelian perspective, however, $\Box p$, $\Diamond p \wedge \Diamond \neg p$ and $\Box \neg p$ are all contrary to each other. Since these formulas lie on a single line in the Hasse hexagon in Fig. 2c, the contrariety edges between them would overlap and would thus not be visually discernible from each other; this is a grave violation of the apprehension principle. The Aristotelian hexagon in Fig. 1c solves this problem by moving $\Diamond p \wedge \Diamond \neg p$ away from the horizontal line between $\Box p$ and $\Box \neg p$: the three contrariety edges now form a triangle and are thus clearly discernible. Of course, the price that has to be paid for achieving this is that the resulting diagram mixes the levels and no longer has a clear entailment direction. However, these properties correspond to the structure of the *entailment ordering*, so by the principle of information selection, it is no problem for an *Aristotelian* diagram to distort them in order to better visualize the *Aristotelian* relations.

4 A Unified Account: Projections of Hypercubes

We now begin with the development of a unified perspective on Aristotelian and Hasse diagrams, by showing how both types of diagrams can be seen as vertex-first projections of n-dimensional hypercubes. This development will be carried out in full generality (for arbitrary n), using some basic tools from linear algebra [36]. Concrete applications to the Aristotelian/Hasse hexagons ($n = 3$) and the Aristotelian/Hasse RDHs ($n = 4$) will be discussed in the next sections.

We will restrict ourselves to Aristotelian diagrams that represent all formulas of a given finite Boolean algebra (except for $\bot$ and $\top$, of course; cf. supra). This restriction is harmless, since every Aristotelian diagram that is not Boolean closed can be embedded inside one that is.[8] It is well-known that every finite Boolean algebra $\mathbb{B}_n$ can be represented as the powerset of a finite set $\{1, \ldots, n\}$,

[8] For example, the Aristotelian square in Fig. 1a can be embedded inside the Aristotelian hexagon in Fig. 1b, and the Aristotelian octagon in Fig. 1c can be embedded inside the Aristotelian RDH in Fig. 3a.

or equivalently, as the set $\{0,1\}^n$ of all *bitstrings* of length n [37, 38]. The latter representation is the most convenient for our purposes, and will thus be used.

It is well-known that the Boolean algebra $\mathbb{B}_n$ can be represented as a hypercube $\mathcal{C}_n$ in n-dimensional Euclidean space $\mathbb{R}^n$ [29, 30]. We now argue that this hypercube is a Hasse diagram for $\mathbb{B}_n$.[9] Consider a coordinate mapping $c\colon \{0,1\}^n \to \mathbb{R}^n$, which maps each bitstring $\varphi \in \{0,1\}^n$ onto its coordinates $c(\varphi) \in \mathbb{R}^n$.[10] It will be convenient to assume that c maps the bits 1 and 0 to the coordinates 1 and -1, respectively—e.g. $c(11010) = (1,1,-1,1,-1)$. The resulting hypercube is centered around the origin $(0,\dots,0)$ of $\mathbb{R}^n$, with central symmetry representing logical negation: $c(\neg\varphi) = -1 \cdot c(\varphi)$, i.e. $\neg\varphi$ is diametrically opposed to φ. The general direction of entailment runs from $\bot$ to $\top$, and thus corresponds to the vector $c(\top) - c(\bot) = (2,\dots,2) \sim (1,\dots,1)$.[11] Any $(n-1)$-dimensional hyperplane orthogonal to this direction has an equation of the form $x_1 + \cdots + x_n = a$. For any bitstring $\varphi \in L_k$ $(0 \leq k \leq n)$, it holds that φ consists of k 1-bits and $n-k$ 0-bits, and hence $\sum_{i=1}^{i=n} c(\varphi)_i = 2k - n$; i.e. $c(\varphi)$ lies on the hyperplane with equation $x_1 + \cdots + x_n = 2k - n$. The level L_k of $\mathbb{B}_n$ thus corresponds to a hyperplane in $\mathbb{R}^n$ that is orthogonal to the entailment direction vector $(1,\dots,1)$.

The Boolean algebra $\mathbb{B}_n$ has 2^n bitstrings, or equivalently, $\frac{2^n}{2} = 2^{n-1}$ pairs of contradictory bitstrings $(\varphi, \neg\varphi)$. Hence, its hypercube representation $\mathcal{C}_n$ has 2^{n-1} pairs of diametrically opposed vertices $(c(\varphi), c(\neg\varphi))$. Each of these pairs defines a direction vector $\mathbf{d}_{\varphi,\neg\varphi} := c(\varphi) - c(\neg\varphi) = c(\varphi) - (-c(\varphi)) = 2c(\varphi) \sim c(\varphi)$. The vector $\mathbf{d}_{\varphi,\neg\varphi}$ can be taken as the projection axis for a vertex-first projection $\Pi_{\varphi,\neg\varphi}$. We will focus on two such projections. The first one is $\Pi_{\top,\bot}$. The second one is harder to describe in general: it is of the form $\Pi_{\gamma,\neg\gamma}$ for some γ near the 'middle' of $\mathbb{B}_n$ (i.e. in the level L_k where $k = \lceil \frac{n}{2} \rceil$); this will become clearer in the concrete case studies. We will also make use of a linear transformation $T\colon \mathbb{R}^n \to \mathbb{R}^n$ that maps $c(\top)$ onto $c(\gamma)$; the matrix representation of T is a diagonal matrix that has the components of $c(\gamma)$ on its diagonal (i.e. $M_{i,i} = c(\gamma)_i$ and $M_{i,j} = 0$ for $1 \leq i \neq j \leq n$). Note that $T \cdot T = I_n$, and thus $T^{-1} = T$.

The projection axis of $\Pi_{\top,\bot}$ is $\mathbf{d}_{\top,\bot} = (1,\dots,1)$. This is a projection onto the $(n-1)$-dimensional hyperplane that goes through the origin and is orthogonal to $\mathbf{d}_{\top,\bot}$, which has the equation $x_1 + \cdots + x_n = 0$. It is possible to choose $n-1$

[9] Since Hasse diagrams can represent all Aristotelian relations, the hypercube is not only a Hasse diagram, but also an Aristotelian diagram. This dual perspective corresponds exactly to the two projections $\Pi_{\top,\bot}$ and $\Pi_{\gamma,\neg\gamma}$ introduced below.

[10] We thus identify the hypercube $\mathcal{C}_n$ with its vertices, and 'ignore' its edges, faces, etc. This is unproblematic, since the latter are linearly generated by the vertices, and all transformations that will be applied to the hypercube are linear transformations. For example, the edge between vertices $\mathbf{x}$ and $\mathbf{y}$ is $E = \{\mathbf{x} + \lambda(\mathbf{y} - \mathbf{x}) \mid \lambda \in [0,1]\}$; for any linear transformation L, it holds that $L[E] = \{L(\mathbf{z}) \mid \mathbf{z} \in E\} = \{L(\mathbf{x}) + \lambda(L(\mathbf{y}) - L(\mathbf{x})) \mid \lambda \in [0,1]\}$, i.e. $L[E]$ is exactly the edge between $L(\mathbf{x})$ and $L(\mathbf{y})$.

[11] For direction vectors $\mathbf{x}, \mathbf{y} \in \mathbb{R}^n$, we write $\mathbf{x} \sim \mathbf{y}$ iff $\mathbf{x}$ and $\mathbf{y}$ are identical up to a scalar λ (i.e. $\mathbf{x} = \lambda\mathbf{y}$). After all, we are only interested in the *direction* of these vectors, not in their particular *magnitude*.

pairwise orthogonal vectors $\rho_1, \ldots, \rho_{n-1}$ in this hyperplane.[12] The matrix that contains these vectors as rows is the matrix representation of $\Pi_{\top,\bot}$. It is easy to show that for the matrix representation of $\Pi_{\gamma,\neg\gamma}$, we can take $\Pi_{\gamma,\neg\gamma} := \Pi_{\top,\bot} \cdot T$. Since $T = T^{-1}$, it immediately follows that $\Pi_{\top,\bot} = \Pi_{\gamma,\neg\gamma} \cdot T$.

We now study the result of applying the vertex-first projection $\Pi_{\top,\bot}$ to the hypercube $\mathcal{C}_n$. Since $c(\neg\varphi) = -c(\varphi)$ and $\Pi_{\top,\bot}$ is a linear transformation, it follows that $\Pi_{\top,\bot}(c(\neg\varphi)) = \Pi_{\top,\bot}(-c(\varphi)) = -\Pi_{\top,\bot}(c(\varphi))$, i.e. $\Pi_{\top,\bot}[\mathcal{C}_n]$ is centered around the origin of $\mathbb{R}^{n-1}$, with central symmetry representing negation. Furthermore, since $c(\top)$ and $c(\bot)$ lie along the direction $\mathbf{d}_{\top,\bot}$ of the projection axis, it follows that $\Pi_{\top,\bot}(c(\top)) = \Pi_{\top,\bot}(c(\bot)) = (0, \ldots, 0) \in \mathbb{R}^{n-1}$. Note that this observation perfectly explains the claim that in an Aristotelian diagram, $\top$ and $\bot$ coincide in the diagram's center of symmetry [27, 33]. Next, recall that the hypercube $\mathcal{C}_n$ is a Hasse diagram, with general entailment direction from $c(\bot)$ to $c(\top)$, i.e. $\mathbf{d}_{\top,\bot}$. Since this direction is exactly the projection axis of $\Pi_{\top,\bot}$, it follows that in $\Pi_{\top,\bot}[\mathcal{C}_n]$ the edges no longer share a common entailment direction: the component of the direction vector that they shared has been 'projected away'. To make this more concrete, Fig. 4a provides an example for a projection $\pi\colon \mathbb{R}^2 \to \mathbb{R}^1$. Note that the vectors $\mathbf{a}, \mathbf{b} \in \mathbb{R}^2$ have more or less the same direction, viz. vertically upwards. However, if we define π to be the projection along exactly this vertical direction, then we see that $\pi(\mathbf{a})$ and $\pi(\mathbf{b})$ do not share the same direction at all (the vertical component that they shared has been projected away). Finally, also recall that $\mathcal{C}_n$ represents the levels L_k of $\mathbb{B}_n$ by means of hyperplanes that are orthogonal to $\mathbf{d}_{\top,\bot}$. However, in $\Pi_{\top,\bot}[\mathcal{C}_n]$, the levels will be 'mixed', since the distance (along $d_{\top,\bot}$) that separated them has been 'projected away'. As an illustration, consider Fig. 4b: the points $\mathbf{a}$ and $\mathbf{b}$ belong to some level L_k, and the points $\mathbf{c}$ and $\mathbf{d}$ belong to a different ('higher') level L_m; thus, $\mathbf{a}$ and $\mathbf{b}$ are both 'below' $\mathbf{c}$ and $\mathbf{d}$. However, when we consider their projections, we see that the levels have been completely 'mixed': $\pi(\mathbf{a})$ lies between $\pi(\mathbf{c})$ and $\pi(\mathbf{d})$, while $\pi(\mathbf{d})$ lies between $\pi(\mathbf{a})$ and $\pi(\mathbf{b})$.

We now consider the other vertex-first projection of the hypercube: $\Pi_{\gamma,\neg\gamma}[\mathcal{C}_n]$. Since the direction of the projection axis $\mathbf{d}_{\gamma,\neg\gamma}$ does *not* coincide with the general entailment direction $\mathbf{d}_{\top,\bot}$ of $\mathcal{C}_n$, matters are much simpler in this case. Since $\mathcal{C}_n$ is a Hasse diagram and thus all its edges share a general entailment direction $\mathbf{d}_{\top,\bot}$, it follows that $\Pi_{\gamma,\neg\gamma}[\mathcal{C}_n]$ also has a general entailment direction, viz. $\Pi_{\gamma,\neg\gamma}(\mathbf{d}_{\top,\bot})$, which runs from $\Pi_{\gamma,\neg\gamma}(c(\bot))$ to $\Pi_{\gamma,\neg\gamma}(c(\top))$. However, one problem seems to remain: $\Pi_{\gamma,\neg\gamma}$ maps the formulas γ and $\neg\gamma$ to the origin of $\mathbb{R}^{n-1}$. This problem can easily be solved, but the details are highly dependent on the concrete case (e.g. it matters whether n is odd or even), and will thus be postponed to the concrete case studies in the next sections.

In sum, the discussion above shows that $\Pi_{\top,\bot}[\mathcal{C}_n]$ and $\Pi_{\gamma,\neg\gamma}[\mathcal{C}_n]$ are resp. an Aristotelian diagram and a Hasse diagram of the Boolean algebra $\mathbb{B}_n$. There is thus a deep connection between Aristotelian and Hasse diagrams: both can be seen as vertex-first projections of one and the same hypercube $\mathcal{C}_n$. Additionally,

[12] In the case studies in the next sections, we will show that it is often possible to choose these vectors in particularly elegant ways.

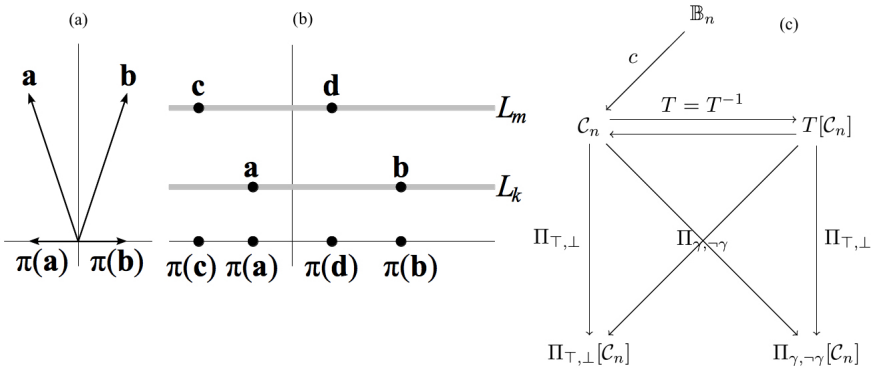

Fig. 4. The effects of projecting along the entailment direction: (a) loss of a shared entailment direction and (b) 'mixing' of levels. Part (c) is a commutative diagram containing the various linear transformations studied in this section.

this viewpoint yields a unified explanation of the various dissimilarities between both types of diagrams (as discussed in Section 3), by showing how they are merely different manifestations of the same underlying process, viz. projecting the Hasse diagram $\mathcal{C}_n$ along its own general entailment direction. Finally, recalling that $\Pi_{\gamma,\neg\gamma} = \Pi_{\top,\bot} \cdot T$ and $\Pi_{\top,\bot} = \Pi_{\gamma,\neg\gamma} \cdot T$, we also have a way to move back and forth between the Aristotelian diagram $\Pi_{\top,\bot}[\mathcal{C}_n]$ and the Hasse diagram $\Pi_{\gamma,\neg\gamma}[\mathcal{C}_n]$, which is summarized by the commutative diagram in Fig. 4c.

5 Case Study I: Hexagons as Projections of the Cube

We will now illustrate the unified account of Aristotelian and Hasse diagrams that was introduced in the previous section, by applying it to some small Boolean algebras. In this section we consider $\mathbb{B}_3$, in Section 6 we will look at $\mathbb{B}_4$.

The Boolean algebra $\mathbb{B}_3$ is represented as a cube $\mathcal{C}_3$ in three-dimensional Euclidean space $\mathbb{R}^3$. This is done by the 'conventional' coordinate mapping $c\colon \{0,1\}^3 \to \mathbb{R}^3$; see Fig. 5a and the $c(\varphi)$-row in Table 1 at the end of this section. The general entailment direction goes from $c(\bot)$ to $c(\top)$, and is thus $c(\top) - (\bot) = (1,1,1) - (-1,-1,-1) = (2,2,2) \sim (1,1,1)$. We will consider two vertex-first projections of $\mathcal{C}_3$. The first one, $\Pi_{\top,\bot}$, is along the direction $\mathbf{d}_{\top,\bot} = (1,1,1)$, and onto the projection plane $x+y+z = 0$ (which is orthogonal to $\mathbf{d}_{\top,\bot}$). For the second one, $\Pi_{\gamma,\neg\gamma}$, we choose $\gamma := 101$; this projection is thus along $\mathbf{d}_{\gamma,\neg\gamma} = c(\gamma) - c(\neg\gamma) = (1,-1,1) - (-1,1,-1) = (2,-2,2) \sim (1,-1,1)$, and onto the projection plane $x - y + z = 0$ (which is orthogonal to $\mathbf{d}_{\gamma,\neg\gamma}$). The projection axes and projection planes of $\Pi_{\top,\bot}$ and $\Pi_{\gamma,\neg\gamma}$ are shown in Fig. 5b and Fig. 5c, respectively. The linear transformation T which maps $c(\top) = (1,1,1)$ onto $c(\gamma) = (1,-1,1)$ corresponds to a reflection over the $(x-z)$-plane (compare Fig. 5b and Fig. 5c); it is described by a 3×3 diagonal matrix with 1, -1 and 1 on its diagonal. (The effect of T on all points of $\mathcal{C}_3$ is described in the $T(c(\varphi))$-row

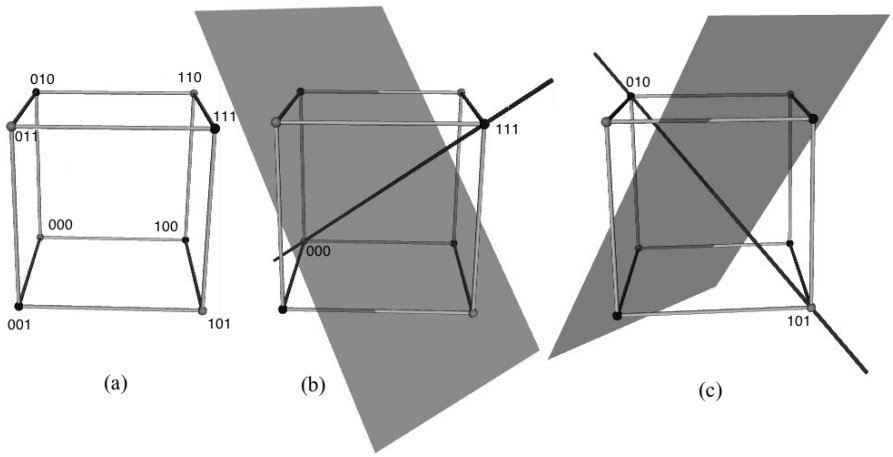

Fig. 5. (a) The cube $\mathcal{C}_3$ with its bitstring decoration; (b) the projection axis and projection plane of $\Pi_{\top,\bot}$; (c) the projection axis and projection plane of $\Pi_{\gamma,\neg\gamma}$

of Table 1.) The matrix representations of the vertex-first projections are

$$\Pi_{\top,\bot} = \begin{pmatrix} \frac{-\sqrt{3}}{4} & 0 & \frac{\sqrt{3}}{4} \\ \frac{1}{4} & \frac{-1}{2} & \frac{1}{4} \end{pmatrix} \quad \text{and} \quad \Pi_{\gamma,\neg\gamma} = \begin{pmatrix} \frac{-\sqrt{3}}{4} & 0 & \frac{\sqrt{3}}{4} \\ \frac{1}{4} & \frac{1}{2} & \frac{1}{4} \end{pmatrix}.$$

Note that the rows of $\Pi_{\top,\bot}$ are two orthogonal vectors that lie in the plane $x+y+z=0$, i.e. the projection plane of $\Pi_{\top,\bot}$. Similarly, the rows of $\Pi_{\gamma,\neg\gamma}$ are two orthogonal vectors that lie in the plane $x-y+z=0$, i.e. the projection plane of $\Pi_{\gamma,\neg\gamma}$. Finally, note that the rows of $\Pi_{\gamma,\neg\gamma}$ are the result of applying the linear transformation T to the corresponding rows of $\Pi_{\top,\bot}$, and thus $\Pi_{\gamma,\neg\gamma} = \Pi_{\top,\bot} \cdot T$.

When the vertex-first projection $\Pi_{\top,\bot}$ is applied to (all points of) the cube $\mathcal{C}_3$, the result is a regular hexagon that is centered around the origin $(0,0)$; this hexagon is shown in Fig. 6a and its concrete coordinates can be found in the $\Pi_{\top,\bot}(c(\varphi))$-row of Table 1. Although the hexagon does not by itself contain any logical relation, it is clear that it is essentially an *Aristotelian diagram* (compare with Fig. 1b). First of all, the non-contingent formulas $\top = 111$ and $\bot = 000$ coincide in the hexagon's center of symmetry. Secondly, the hexagon does not have a single direction of entailment (in contrast, $\mathcal{C}_3$ does have such a direction, viz. $\mathbf{d}_{\top,\bot}$). Finally, the levels L_k have been 'mixed'; for example, the bitstrings of L_1 and those of L_2 form two interlocking triangles (in contrast, in $\mathcal{C}_3$ the levels L_1 and L_2 are represented by means of the planes $x+y+z=-1$ and $x+y+z=1$, respectively).

We now turn to the second projection, viz. $\Pi_{\gamma,\neg\gamma}$. The result is again a regular hexagon that is centered around the origin; this hexagon is shown in Fig. 6b and its concrete coordinates can be found in the $\Pi_{\gamma,\neg\gamma}(c(\varphi))$-row of Table 1. Although this hexagon has $\bot = 000$ at its lowest vertex and $\top = 111$ at its highest, and

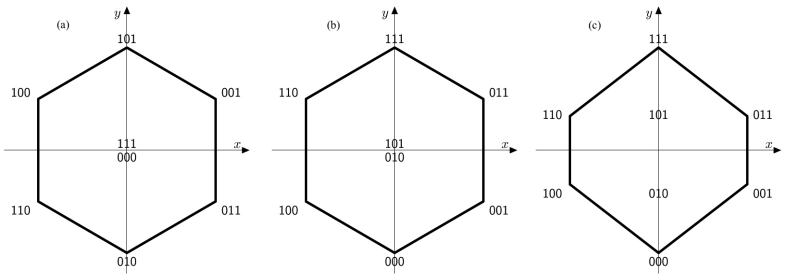

Fig. 6. (a) $\Pi_{\top,\bot}[\mathcal{C}_3]$, (b) $\Pi_{\gamma,\neg\gamma}[\mathcal{C}_3]$, (c) $\Pi^{1/3}_{\gamma,\neg\gamma}[\mathcal{C}_3]$

Table 1. The elements of $\mathbb{B}_3$, $\mathcal{C}_3$, $\Pi_{\top,\bot}[\mathcal{C}_3]$, $\Pi_{\gamma,\neg\gamma}[\mathcal{C}_3]$ and $\Pi^{1/3}_{\gamma,\neg\gamma}[\mathcal{C}_3]$

φ	111	110	101	011	100	010	001	000
$c(\varphi)$	(1,1,1)	(1,1,-1)	(1,-1,1)	(-1,1,1)	(1,-1,-1)	(-1,1,-1)	(-1,-1,1)	(-1,-1,-1)
$T(c(\varphi))$	(1,-1,1)	(1,-1,-1)	(1,1,1)	(-1,-1,1)	(1,1,-1)	(-1,-1,-1)	(-1,1,1)	(-1,1,-1)
$\Pi_{\top,\bot}(c(\varphi))$	(0,0)	$(-\frac{\sqrt{3}}{2},-\frac{1}{2})$	(0,1)	$(\frac{\sqrt{3}}{2},-\frac{1}{2})$	$(-\frac{\sqrt{3}}{2},\frac{1}{2})$	(0,-1)	$(\frac{\sqrt{3}}{2},\frac{1}{2})$	(0,0)
$\Pi_{\gamma,\neg\gamma}(c(\varphi))$	(0,1)	$(-\frac{\sqrt{3}}{2},\frac{1}{2})$	(0,0)	$(\frac{\sqrt{3}}{2},\frac{1}{2})$	$(-\frac{\sqrt{3}}{2},-\frac{1}{2})$	(0,0)	$(\frac{\sqrt{3}}{2},-\frac{1}{2})$	(0,-1)
$\Pi^{1/3}_{\gamma,\neg\gamma}(c(\varphi))$	(0,1)	$(-\frac{\sqrt{3}}{2},\frac{1}{3})$	$(0,\frac{1}{3})$	$(\frac{\sqrt{3}}{2},\frac{1}{3})$	$(-\frac{\sqrt{3}}{2},-\frac{1}{3})$	$(0,-\frac{1}{3})$	$(\frac{\sqrt{3}}{2},-\frac{1}{3})$	(0,-1)

also has a general direction of entailment—viz. vertically upwards—, it is not a true Hasse diagram, since the bitstrings 101 and 010 coincide in the center, and thus the levels L_1 and L_2 are not represented uniformly.

However, this problem can be solved if we introduce a small *perturbation* ε to the vertex-first projection $\Pi_{\gamma,\neg\gamma}$, thus obtaining the 'quasi-projection' $\Pi^{\varepsilon}_{\gamma,\neg\gamma}$. This quasi-projection is defined in such a way that if $\varepsilon = 0$, then $\Pi^{\varepsilon}_{\gamma,\neg\gamma} = \Pi_{\gamma,\neg\gamma}$. For our current purposes, however, we will particularly be interested in the case $\varepsilon = \frac{1}{3}$. Here is the general definition, and the special case $\varepsilon = \frac{1}{3}$:

$$\Pi^{\varepsilon}_{\gamma,\neg\gamma} = \begin{pmatrix} \frac{-\sqrt{3}}{4} & 0 & \frac{\sqrt{3}}{4} \\ \frac{1+\varepsilon}{4} & \frac{1-\varepsilon}{2} & \frac{1+\varepsilon}{4} \end{pmatrix}, \qquad \Pi^{1/3}_{\gamma,\neg\gamma} = \begin{pmatrix} \frac{-\sqrt{3}}{4} & 0 & \frac{\sqrt{3}}{4} \\ \frac{1}{3} & \frac{1}{3} & \frac{1}{3} \end{pmatrix}.$$

Fig. 6c shows the hexagon that results from applying this quasi-projection to the cube $\mathcal{C}_3$; its coordinates can be found in the $\Pi^{1/3}_{\gamma,\neg\gamma}(c(\varphi))$-row of Table 1. Although the hexagon is no longer regular, it can properly be called a *Hasse diagram* (compare with Fig. 2c). It represents $\bot = 000$ and $\top = 111$ at resp. its lowest and highest point. Furthermore, it has a general entailment direction, viz. vertically upward. Finally, the levels are represented by lines that are horizontal (and thus orthogonal to the general entailment direction); for example, L_1 and L_2 correspond to the horizontal lines $y = -\frac{1}{3}$ and $y = \frac{1}{3}$, respectively.

6 Case Study II: RDHs as Projections of the Hypercube

As a second illustration of the unified account described in Section 4, we will now apply it to $\mathbb{B}_4$. This Boolean algebra is represented as a four-dimensional hypercube $\mathcal{C}_4 \subset \mathbb{R}^4$. We again employ the 'conventional' coordinate mapping $c\colon \{0,1\}^4 \to \mathbb{R}^4$; see the $c(\varphi)$-row in Table 2. The general entailment direction in this hypercube is $(1,1,1,1)$. We consider two vertex-first projections of $\mathcal{C}_4$. The first one, $\Pi_{\top,\bot}$, is along the direction $\mathbf{d}_{\top,\bot} = (1,1,1,1)$, and onto the projection plane $x+y+z+u=0$ (which is orthogonal to $\mathbf{d}_{\top,\bot}$). For the second one, $\Pi_{\gamma,\neg\gamma}$, we choose $\gamma := 1001$; this projection is thus along $\mathbf{d}_{\gamma,\neg\gamma} = (1,-1,-1,1)$, and onto the projection plane $x-y-z+u=0$ (which is orthogonal to $\mathbf{d}_{\gamma,\neg\gamma}$). The linear transformation T which maps $c(\top) = (1,1,1,1)$ onto $c(\gamma) = (1,-1,-1,1)$ is described by a 4×4 diagonal matrix with 1, -1, -1 and 1 on its diagonal; see the $T(c(\varphi))$-row of Table 2. The matrix representations of the projections are

$$\Pi_{\top,\bot} = \begin{pmatrix} -0.5 & -0.5 & 0.5 & 0.5 \\ 0.5 & -0.5 & -0.5 & 0.5 \\ 0.5 & -0.5 & 0.5 & -0.5 \end{pmatrix} \quad \text{and} \quad \Pi_{\gamma,\neg\gamma} = \begin{pmatrix} -0.5 & 0.5 & -0.5 & 0.5 \\ 0.5 & 0.5 & 0.5 & 0.5 \\ 0.5 & 0.5 & -0.5 & -0.5 \end{pmatrix}.$$

The rows of $\Pi_{\top,\bot}$ are pairwise orthogonal vectors that lie in the plane $x+y+z+u=0$, i.e. the projection plane of $\Pi_{\top,\bot}$; similar remarks apply to $\Pi_{\gamma,\neg\gamma}$.

When the vertex-first projection $\Pi_{\top,\bot}$ is applied to the hypercube $\mathcal{C}_4$, the result is an RDH that is centered around the origin $(0,0,0)$. This RDH was already shown in Fig. 3a; its concrete coordinates can be found in the $\Pi_{\top,\bot}(c(\varphi))$-row of Table 2. This RDH is essentially an *Aristotelian diagram*: the non-contingent formulas $\top = 1111$ and $\bot = 0000$ coincide in the RDH's center of symmetry, the RDH does not have a single direction of entailment, and the levels of $\mathbb{B}_4$ have been 'mixed'; e.g. the bitstrings of L_1 and L_3 form two interlocking tetrahedrons.

We now turn to the second projection, viz. $\Pi_{\gamma,\neg\gamma}$. The result is again an RDH that is centered around the origin; its concrete coordinates can be found in the $\Pi_{\gamma,\neg\gamma}(c(\varphi))$-row of Table 2. This RDH is not a true Hasse diagram, since the bitstrings 1001 and 0110 coincide. However, this problem can be solved by introducing a small *perturbation* ε to $\Pi_{\gamma,\neg\gamma}$. The resulting 'quasi-projection' $\Pi^{\varepsilon}_{\gamma,\neg\gamma}$ is defined in such a way that if $\varepsilon = 0$, then $\Pi^{\varepsilon}_{\gamma,\neg\gamma} = \Pi_{\gamma,\neg\gamma}$. Here is the general definition, and the special case $\varepsilon = \frac{1}{10} = 0.1$:

$$\Pi^{\varepsilon}_{\gamma,\neg\gamma} = \begin{pmatrix} -0.5 & 0.5+\varepsilon & -0.5+\varepsilon & 0.5 \\ 0.5 & 0.5 & 0.5 & 0.5 \\ 0.5 & 0.5 & -0.5 & -0.5 \end{pmatrix}, \quad \Pi^{1/10}_{\gamma,\neg\gamma} = \begin{pmatrix} -0.5 & 0.6 & -0.4 & 0.5 \\ 0.5 & 0.5 & 0.5 & 0.5 \\ 0.5 & 0.5 & -0.5 & -0.5 \end{pmatrix}.$$

Fig. 3b shows the RDH that results from applying this quasi-projection to the hypercube $\mathcal{C}_4$; its coordinates are in the $\Pi^{1/10}_{\gamma,\neg\gamma}(c(\varphi))$-row of Table 2. This RDH is a proper *Hasse diagram*: it represents $\bot = 0000$ and $\top = 1111$ at resp. its lowest and highest point, it has a general entailment direction (viz. vertically upward), and finally, the levels are represented by planes that are horizontal (and thus orthogonal to the general entailment direction); for example, L_1, L_2 and L_3 correspond to the horizontal planes $y=-1$, $y=0$ and $y=1$, respectively.

Table 2. The elements of $\mathbb{B}_4$, $\mathcal{C}_4$, $\Pi_{\top,\bot}[\mathcal{C}_4]$, $\Pi_{\gamma,\neg\gamma}[\mathcal{C}_4]$ and $\Pi^{1/10}_{\gamma,\neg\gamma}[\mathcal{C}_4]$. For reasons of space, the table lists only 8 of the 16 bitstrings of $\mathbb{B}_4$; it can be completed by adding their 8 negations, and recalling that $c(\neg\varphi) = -c(\varphi)$, $T(c(\neg\varphi)) = -T(c(\varphi))$, $\Pi_{\top,\bot}(c(\neg\varphi)) = -\Pi_{\top,\bot}(c(\varphi))$, $\Pi_{\gamma,\neg\gamma}(c(\neg\varphi)) = -\Pi_{\gamma,\neg\gamma}(c(\varphi))$ and $\Pi^{1/10}_{\gamma,\neg\gamma}(c(\neg\varphi)) = -\Pi^{1/10}_{\gamma,\neg\gamma}(c(\varphi))$.

φ	1111	1110	1101	1011	0111	1100	1010	1001
$c(\varphi)$	(1,1,1,1)	(1,1,1,-1)	(1,1,-1,1)	(1,-1,1,1)	(-1,1,1,1)	(1,1,-1,-1)	(1,-1,1,-1)	(1,-1,-1,1)
$T(c(\varphi))$	(1,-1,-1,1)	(1,-1,-1,-1)	(1,-1,1,1)	(1,1,-1,1)	(-1,-1,-1,1)	(1,-1,1,-1)	(1,1,-1,-1)	(1,1,1,1)
$\Pi_{\top,\bot}(c(\varphi))$	(0,0,0)	(-1,-1,1)	(-1,1,-1)	(1,1,1)	(1,-1,-1)	(-2,0,0)	(0,0,2)	(0,2,0)
$\Pi_{\gamma,\neg\gamma}(c(\varphi))$	(0,2,0)	(-1,1,1)	(1,1,1)	(-1,1,-1)	(1,1,-1)	(0,0,2)	(-2,0,0)	(0,0,0)
$\Pi^{1/10}_{\gamma,\neg\gamma}(c(\varphi))$	(0.2,2,0)	(-0.8,1,1)	(1,1,1)	(-1,1,-1)	(1.2,1,-1)	(0,0,2)	(-2,0,0)	(-0.2,0,0)

7 Conclusion

In this paper we have explored the relationship between two important types of diagrams for representing logical relations between formulas, viz. Aristotelian and Hasse diagrams. After briefly discussing some obvious similarities and dissimilarities, we argued that there exists a deep connection between both types of diagrams. On a *visual-cognitive* level, we showed that their dissimilarities can perfectly be explained in terms of general principles of diagram design, such as congruity, apprehension and information selection. On a more abstract *geometrical* level, we showed that pairs of Boolean closed Aristotelian and Hasse diagrams can be seen as different vertex-first projections of one and the same hypercube, thereby obtaining a unified explanation of their dissimilarities.

In future work, we plan to use this geometrical account in the search for adequate Aristotelian/Hasse diagrams for larger Boolean algebras. For example, although there are currently no satisfactory diagrams for $\mathbb{B}_5$ in 3D, we know that they certainly exist in 4D, viz. as vertex-first projections of the 5D hypercube.

Acknowledgements The first author is financially supported by a PhD fellowship of the Research Foundation–Flanders (FWO).

References

1. Howse, J., Stapleton, G., Taylor, J.: Spider diagrams. LMS Journal of Computation and Mathematics 8, 145–194 (2005)
2. Rodgers, P.: A survey of Euler diagrams. J. of Visual Lang. & Comp. (in press)
3. Shin, S.J.: The Iconic Logic of Peirce's Graphs. MIT Press (2002)
4. Stapleton, G.: A survey of reasoning systems based on Euler diagrams. Electronic Notes in Theoretical Computer Science 134, 127–151 (2005)
5. Stapleton, G., Howse, J., Rodgers, P.: A graph theoretic approach to general Euler diagram drawing. Theoretical Computer Science 411, 91–112 (2010)
6. Davey, B., Priestley, H.: Introduction to Lattices and Order. Cambridge UP (2002)
7. Demey, L.: Algebraic aspects of duality diagrams. In: Cox, P.T., Plimmer, B., Rodgers, P. (eds.) Diagrams 2012, pp. 300–302. LNCS 7352, Springer (2012)

8. Demey, L.: Structures of oppositions for public announcement logic. In: Béziau, J.Y., Jacquette, D. (eds.) Around and Beyond the Square of Opposition, pp. 313–339. Springer (2012)
9. Moretti, A.: The Geometry of Logical Opposition. Ph.D. thesis, Neuchâtel (2009)
10. Smessaert, H.: Boolean differences between two hexagonal extensions of the logical square of oppositions. In: Cox, P.T., Plimmer, B., Rodgers, P. (eds.) Diagrams 2012, pp. 193–199. LNCS 7352, Springer (2012)
11. Smessaert, H.: The classical Aristotelian hexagon versus the modern duality hexagon. Logica Universalis 6, 171–199 (2012)
12. Smessaert, H., Demey, L.: Logical geometries and information in the square of oppositions. Submitted (2014)
13. Zellweger, S.: Untapped potential in Peirce's iconic notation for the sixteen binary connectives. In: Houser, N., Roberts, D.D., Van Evra, J. (eds.) Studies in the Logic of Charles Peirce, pp. 334–386. Indiana University Press (1997)
14. Hurley, P.J.: A Concise Introduction to Logic (11th ed.). Wadsworth (2012)
15. Bernhard, P.: Visualizations of the square of opposition. Log. Univ. 2, 31–41 (2008)
16. Seuren, P.: The Logic of Language. Oxford University Press (2010)
17. Carnielli, W., Pizzi, C.: Modalities and Multimodalities. Springer (2008)
18. Lenzen, W.: How to square knowledge and belief. In: Béziau, J.Y., Jacquette, D. (eds.) Around and Beyond the Square of Opposition, pp. 305–311. Springer (2012)
19. McNamara, P.: Deontic logic. In: Stanford Encyclopedia of Philosophy (2010)
20. Moretti, A.: The geometry of standard deontic logic. Log. Univ. 3, 19–57 (2009)
21. Blanché, R.: Structures Intellectuelles. Vrin (1966)
22. Jacoby, P.: A triangle of opposites for types of propositions in Aristotelian logic. New Scholasticism 24, 32–56 (1950)
23. Sesmat, A.: Logique II. Les Raisonnements. La syllogistique. Hermann (1951)
24. Béziau, J.Y.: New light on the square of oppositions and its nameless corner. Logical Investigations 10, 218–232 (2003)
25. Ganter, B., Stumme, G., Wille, R. (eds.): Formal Concept Analysis: Foundations and Applications. Springer (2005)
26. Chatti, S., Schang, F.: The cube, the square and the problem of existential import. History and Philosophy of Logic 32, 101–132 (2013)
27. Smessaert, H.: On the 3D visualisation of logical relations. Logica Universalis 3, 303–332 (2009)
28. Smessaert, H., Demey, L.: Logical and geometrical complementarities between Aristotelian diagrams. To appear in the proceedings of Diagrams 2014 (2014)
29. Foldes, S.: A characterization of hypercubes. Discr. Math. 17, 155–159 (1977)
30. Harary, F., Hayes, J.P., Wu, H.J.: A survey of the theory of hypercube graphs. Computers & Mathematics with Applications 15, 277–289 (1988)
31. Kauffman, L.H.: The mathematics of Charles Sanders Peirce. Cybernetics & Human Knowing 8, 79–110 (2001)
32. Flower, J., Stapleton, G., Rodgers, P.: On the drawability of 3D Venn and Euler diagrams. Journal of Visual Languages & Computing (in press)
33. Sauriol, P.: Remarques sur la théorie de l'hexagone logique de Blanché. Dialogue 7, 374—390 (1968)
34. Tversky, B.: Prolegomenon to scientific visualizations. In: Gilbert, J.K. (ed.) Visualization in Science Education, pp. 29–42. Springer (2005)
35. Tversky, B.: Visualizing thought. Topics in Cognitive Science 3, 499–535 (2011)
36. Strang, G.: Introduction to Linear Algebra. Wellesley-Cambridge Press (2009)
37. Givant, S., Halmos, P.: Introduction to Boolean Algebras. Springer (2009)
38. Smessaert, H., Demey, L.: The unreasonable effectiveness of bitstrings in logical geometry. 4th World Congress on the Square of Opposition (2014)